Electronic supplementary materials *Mendeleev Commun.*, 2025, **35**, 586–588

End-group analysis to characterize the ring-opening polymerization of propylene oxalate

Nikolai P. Iakimov, Ekaterina M. Budynina, Evgenii O. Fomin, Alexandra A. Egorova, Anna K. Berkovich, Marina V. Serebriakova, Irina D. Grozdova and Nikolay S. Melik-Nubarov

S1. Materials and Methods

Propylene glycol (Sigma-Aldrich, USA) was dried over molecular sieves 4Å and vacuum distilled. Tetrahydrofuran (THF) (Component-Reaktiv, Russia) was distilled over KOH, refluxed over sodium metal with benzophenone (Sigma-Aldrich), and distilled on the day of the experiment. Pyridine (Component-Reaktiv, Russia) was dried by heating over CaH_2 under reflux and further distillation. Ethanol (Component-Reaktiv, Russia) was dehydrated by heating over CaO (ethanol/CaO mass ratio was 3:1) under reflux, distilled, refluxed over molecular sieves 3Å and redistilled. Oxalyl chloride, tin(II) octoate [$Sn(Oct)_2$, ABCR, Germany], and $CDCl_3$ (CarlRoth, Germany) were used as received.

PrOx was synthesized as previously reported.[S1] The resulting monomer was stored under argon in a desiccator over dry NaOH at 4 °C and was always sampled in the stream of argon. ^{1}H NMR ($CDCl_3$, 600 MHz, Figure S1) δ = 1.49 (d, ^3J = 6.6 Hz, 3H, CH_3), 4.46 (dd, ^2J = 12.7, ^{3}J = 9.0 Hz, 1H, CH_2), 4.53 (dd, ^2J = 12.7, ^3J = 2.6 Hz, ^{1}H, CH_2), 4.99 (dqd, ^3J = 9.0, 6.6, 2.6 Hz, 1H, CH).

The ring-opening polymerization of propylene oxalate was conducted in bulk at 100 °C. An aliquot of monomer (0.1 g, 0.77 mmol) was placed into a flame-dried ampule filled with argon. The ampule was connected to the vacuum line and underwent three pumping and argon filling cycles at 50 °C. The solution of $Sn(Oct)_2$ (0.1 M) containing the appropriate amounts of initiator (benzyl alcohol) in dry THF (50 μL) was introduced into the ampule using a gas-tight syringe (Hamilton Company). The mixed sample was frozen using liquid nitrogen. Then the solvent was removed under vacuum. The ampule was sealed up under reduced pressure and stored at -20 °C. Polymerization was conducted by immersing ampoules in an oil bath maintained at 100 °C for a predefined time interval. The polymerized samples were dissolved in THF and centrifuged for removal of SnC_2O_4 precipitate. Model reaction of propylene oxalate with propylene glycol was performed using the same protocol.

Size-exclusion chromatography of the obtained polymers was performed in THF at 40 °C with a flow rate of 1 mL·min^{-1}. The chromatographic system consisted of Altex pump, Knauer Smartline RI detector, Rheodyne® 7125 Front-Loading Injector, and HR-3 and HR-4 Ultrastyragel columns. The polystyrene standard samples (Waters, USA) were used to calibrate the system.

1D and 2D NMR experiments were conducted using Bruker Avance 600 spectrometer at 303 K. The samples for NMR analysis were dissolved in $CDCl_3$ (Chemical Line, Russia). The chemical shifts δ_H were measured in ppm with respect to the residual protic solvent ($CHCl_3$, δ_H = 7.27 ppm). Content of BnOH in samples was determined by integration of signals at 7.3-7.4 ppm (5H). The oligomers content was determined by the integral intensity of the shoulder at 5.38 ppm. For this purpose, we deconvolved the signal within the 5.25-5.45 ppm region and calculated the ratio of integral intensities of signals at 5.33 (CH of the polymer repeat units) and 5.38 ppm (CH of the oligomers). The number-average polymerization degree P_n(NMR) was calculated according to equation (1) represented in the main text. Concentrations of benzyl, primary and secondary hydroxy end groups were assessed using signals at 7.3-7.4 (5H), 5.05 (1H) and 4.06 (2H), respectively. It is worth noting that this method of P_n(NMR) evaluation is limited by the accuracy of the integration of the end group NMR signals and is not applicable for polyoxalates with P_n greater than 150 ($M_n \sim 2\times10^4$).

The polymers were analyzed by Matrix-Assisted Laser Desorption Ionization Time-Of-Flight mass-spectrometry on UltrafleXtreme MALDI-TOF mass spectrometer (Bruker Daltonics, Bremen, Germany) to detect positive molecular ions (MH^+ or MNa^+ or MK^+) in the range of 100-6000 m/z. For these experiments, 0.5 μL of a sample (4 $mg \cdot mL^{-1}$ of solution in THF) was mixed with 1 μL of 2,5-dihydroxybenzoic acid solution (40 $mg \cdot mL^{-1}$ in water/acetonitrile mixture 7:3). The spectra were recorded in reflector mode, and the accuracy of the monoisotopic mass peak measurement was within 0.2 Da. Mass spectra were processed using FlexAnalysis 3.3 software (Bruker Daltonics, Bremen, Germany).

Glass transition temperature in PPOx was measured using a DSC 204 F1 (Netzsch, Selb, Germany) within the temperature range 213–323 K (heating rate 10 $K \cdot min^{-1}$) in inert atmosphere with argon flow rate 100 $mL \cdot min^{-1}$ in aluminium crucibles.

S2. End-group analysis of products of model reaction using ^{1}H NMR

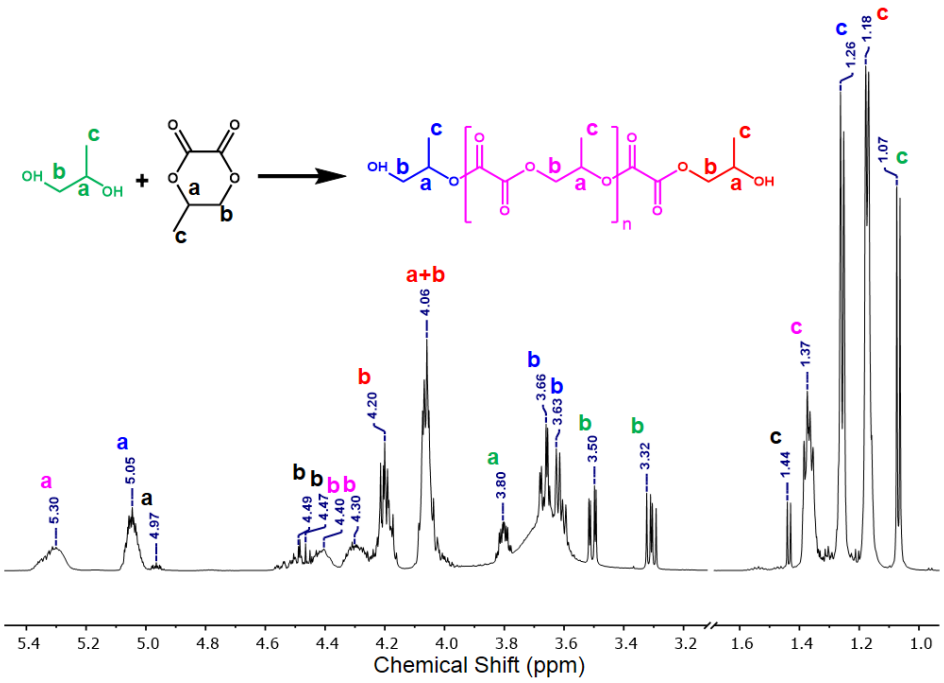

Figure S1. ^{1}H-NMR spectrum of the reaction mixture after reaction of PrOx with equimolar amounts of Pg in the presence of 0.65 % (mol.) $Sn(Oct)_2$, 100 °C, 24 h. a, b, c denote CH, CH_2, and CH_3, respectively. The signal designation for PrOx, PPOx and Pg are black, magenta, and green, respectively. The primary end Pg residues are shown in blue, and the secondary – in red.

Table S1. Chemical shifts and integral intensities of ^{1}H NMR signals of the model reaction products

	δ_{CH3}, ppm (eqv.)	δ_{CH2_1}, ppm (eqv.)	δ_{CH2_2}, ppm (eqv.)	δ_{CH}, ppm (eqv.)
Propylene glycol	1.07 (3.0)	3.31 (1.1)	3.50 (1.2)	3.80 (–)
Monomer	1.44 (3.0)	4.47 (–)	4.49 (–)	4.97 (1.0)
Polymer	1.37 (3.0)	4.30 (1.0)	4.40 (0.8)	5.30 (1.0)
Primary hydroxyl	1.26 (3.0)	3.63 (–)	3.66 (–)	5.05 (1.0)
Secondary hydroxyl	1.18 (3.0)	4.20 (1.2)	4.06 (2.0)	

Chemical shifts, integral intensities and assignments of all signals are summarised in **Table S1**. The signals referred to the polyoxalate repeat units in the middle of chain (**Figure S1, magenta**), Pg (**Figure S1, green**), and the monomer **(Figure S1, black)** were assigned based on spectra presented previously.[S1-S3] The *seven* signals with δ of 5.05, 4.20, 4.06, 3.66, 3.63, 1.26, and 1.18 ppm, can be attributed to terminal links of PPOx.

The common regularity δH(CH) > δH(CH_2) > δH(CH_3) is obeyed for the known spectra of Pg, PPOx, and the monomer. The CH signal of PPOx is a poorly resolved double doublets, while the CH_2 and CH_3 signals are resolved doublets. Because the end Pg fragments are monoesters, signals from their protons should be positioned between the corresponding signals of the free Pg (strong field) and diester of Pg (low field) within the PPOx chain.

Then the positions of signals of CH, CH_2, and CH_3 groups should vary within 3.8-5.3 ppm, 3.3-4.5 ppm, and 1.1-1.6 ppm intervals, respectively. Therefore, the signal of the end group with the highest chemical shift should correspond to methine proton. As this signal is localized in very low field, this CH should be located near the ester group. So, the peak at 5.05 ppm refers to methine protons of Pg with primary OH group (**Figure S1, blue a**). Of the two signals assigned to the CH_3 signals of end groups, signal at 1.26 ppm should be attributed to the same Pg residues with primary hydroxy groups (**Figure S1, blue c**). The doublet at 3.66 and 3.63 ppm located at the pedestal of a broad singlet of probably hydroxyl protons is slightly shifted in respect to signal of methylene protons of the free Pg. Therefore, these signals can be attributed to the CH_2 protons of terminal Pg residues with the primary OH-groups (**Figure S1, blue b**).

The rest signals correspond to protons of terminal Pg residues with secondary OH-groups. When interpreting these signals, it is easiest to attribute the signals of the methyl protons to the signal at 1.18 ppm (red c), which is close to the signals of methyl protons of the free Pg (1.07 ppm).

The situation is more confusing with the signals of methylene and methine protons. Methylene groups should produce a doublet, so the total should be three signals. **Figure S1** shows a complex multiplets at 4.06 ppm and 4.20 ppm that remain unidentified. The total intensity of the signal at 4.06 is nearly twice greater than the signal at 4.20 ppm. This signal seems to be the result of overlapping of the signal of methine and one of two methylene protons of the terminal residues with secondary OH-group (red a+b), while the chemical shift of 4.20 ppm corresponded to the second signal of CH_2 (**Figure S1, red b**).

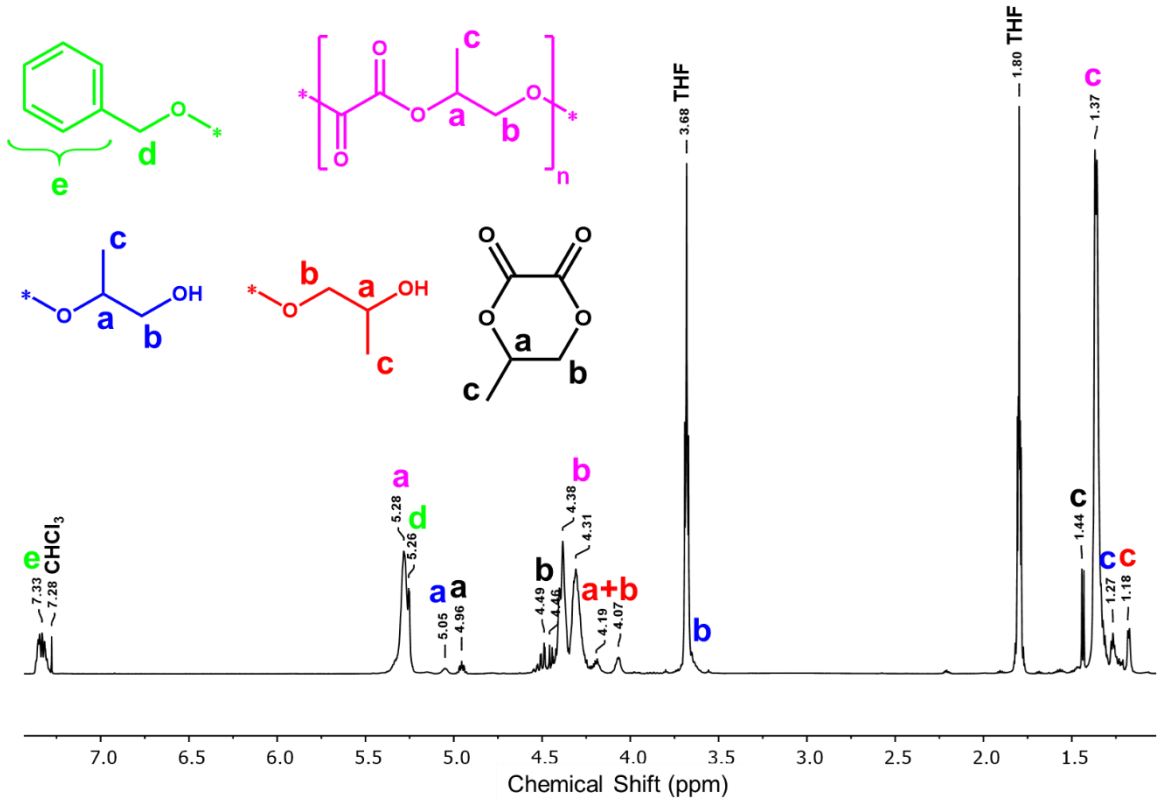

Figure S2. ^{1}H NMR spectrum of the reaction mixture resulting from polymerization of propylene oxalate initiated with BnOH in the presence of $Sn(Oct)_2$ [$C(Sn(Oct)_2]$ = 0.65% (mol.), C(BnOH) = 5.7% (mol.), 100 ^{o}C, 24 h).

S3. End-group analysis of polymerization products by 2D NMR

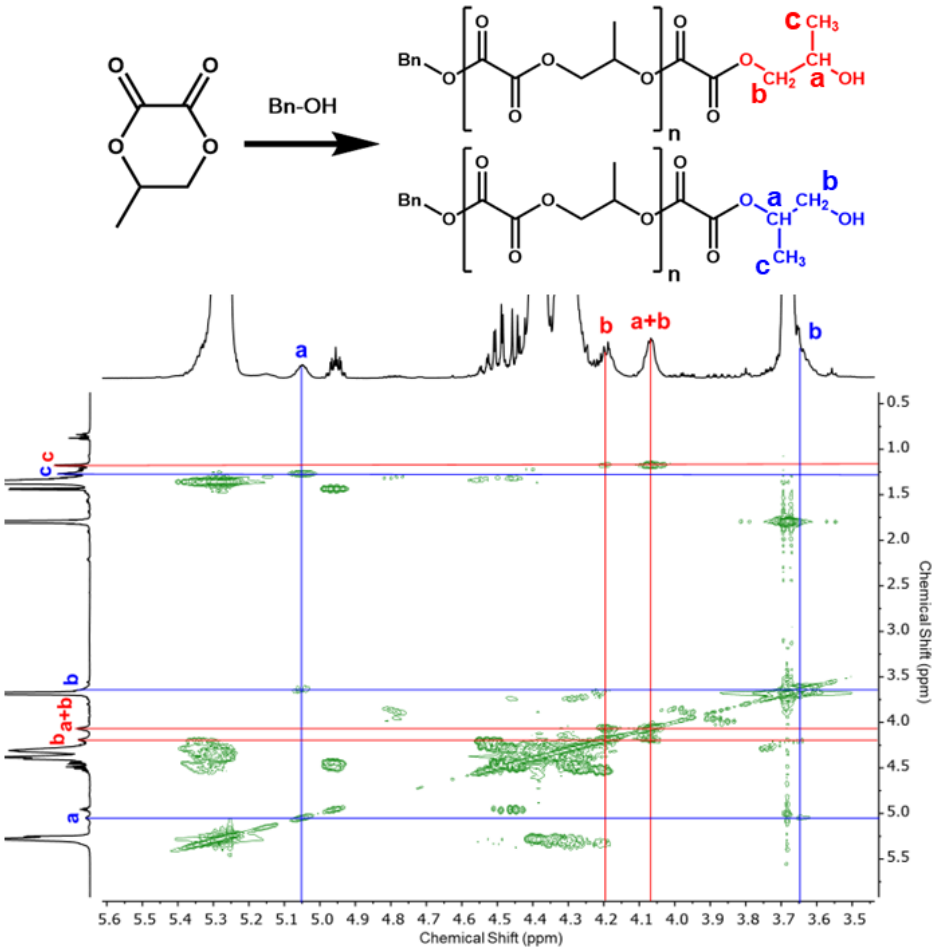

Figure S3. ^{1}H-^{1}H COSY spectrum of reaction mixture resulting from polymerisation of PrOx initiated by BnOH in presence of $Sn(Oct)_2$ [$C(Sn(Oct)_2$] = 0.65 % (mol.), C(BnOH) = 5.7 % (mol.), 100 ^{o}C, 24 h). Blue and red lines indicate cross peaks corresponding to the signals of primary and secondary Pg terminal residues, respectively.

Products of propylene oxalate ROP initiated by BnOH were analysing by ^{1}H-^{1}H COSY NMR. There were several cross peaks related to the terminal Pg residues in the 2D spectrum. The signal attributed to the methine protons of the Pg residues with primary hydroxy group (**Figure S3, blue a**, 5.05 ppm) correlates strongly with the proposed signals of the methylene (**Figure S3, blue b**, 3.66 ppm, overlapping with the THF signal, 3.7 ppm) and methyl (**Figure S3, blue c**, 1.26 ppm) protons. No correlation between methyl and methylene protons was observed.

In the case of the residues with secondary hydroxy group, the signal of methyl protons (**Figure S3, red c**, 1.18 ppm) gave cross peaks with two signals (**Figure S3**, 4.06 and 4.20 ppm). But the correlation with the signal at 4.06 ppm was much stronger, showing that this signal was related to the methine proton neighbouring to methyl group. According to the results of the model experiment, this signal corresponds to 2 protons (**Table S1**), therefore the signal at 4.06 ppm should be attributed to the overlapping signals

of the methine proton and the part of the splitted signal of the methylene protons. Thus, the interpretation of the ^{1}H NMR spectra proposed in Section 2 is in full agreement with the COSY data.

S4. The reason of hydroxy end groups disproportion, estimation of regioregularity of PPOx

In terms of kinetics, the four possible types of propagation reactions can be assigned four constants, k_{ij}, where *i* is the type of attacking hydroxyl [primary (1) or secondary (2)] and *j* is the type of ester bond [formed by a primary (1) or secondary (2) hydroxy group] being broken (**Figure S4a**). Requirement for preferred cleavage of the ester bond formed by the secondary hydroxyl is $k_{12} > k_{11}$, $k_{22} > k_{21}$ (**Figure S4b**). On the contrary, the enhanced reactivity of the primary hydroxy groups explained by higher pK_a and less steric hindrance translates in the following relations between these rate constants: $k_{12} \approx k_{11} > k_{22} \approx k_{21}$. These two cases can be distinguished by the regioregularity of the resultant polymer.

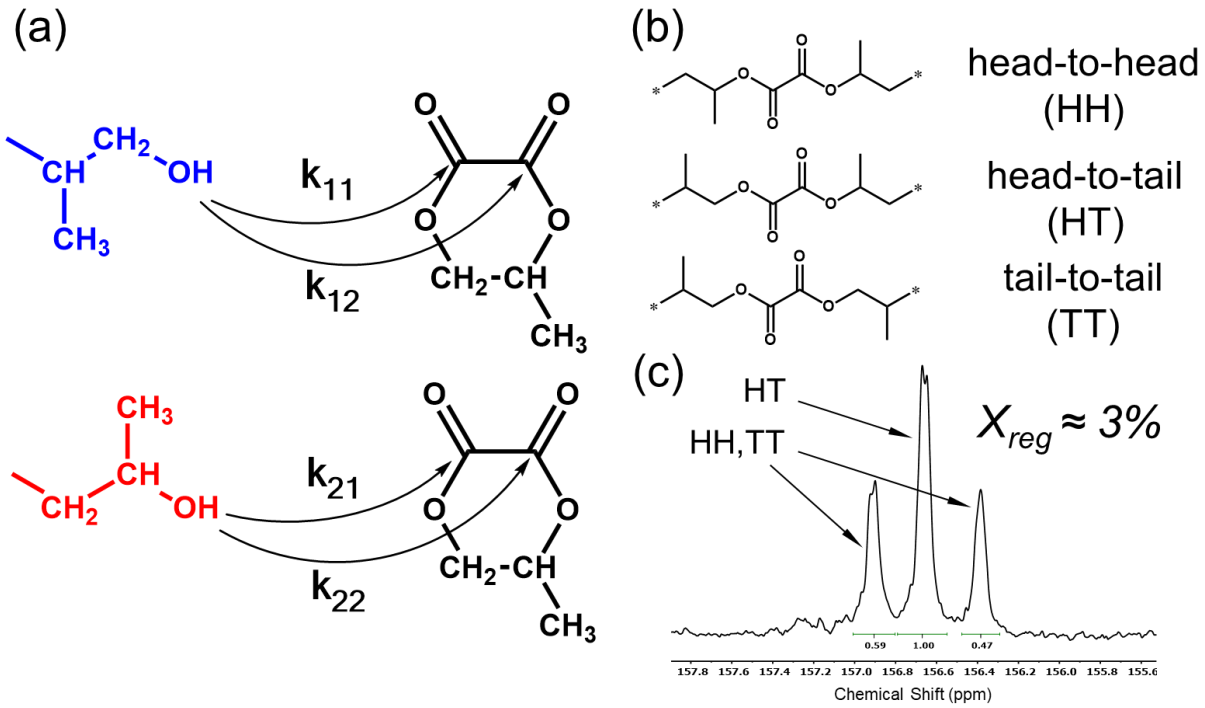

Figure S4. Difference in reactivity of primary and secondary terminal OH-groups and the absence of regioregularity of PPOx. (*a*) Scheme of PrOx ring-opening by primary and secondary hydroxy end groups. (*b*) Structures of three diads which can form in PPOx. (*c*) The fragment of ^{13}C NMR spectra with peaks of carbonyl atoms.

For this purpose, ^{13}C NMR spectroscopy can be used, following the approach commonly used to analyse the regioregularity of polycarbonates from asymmetric derivatives of trimethylene carbonate.[S4-S6] It is known that the ring-opening regioselectivity should leave its mark on the dyad composition of the polymer. The dyad composition is usually described in Head-Tail terms, commonly employed for the description of regioregularity of vinyl polymers. In case of polycarbonates polymerized via ROP, the more substituted carbon is accepted to be "Head" (H), while the less one – "Tail" (T). In the case of PrOx

this translates to the designation of the ester bond with the primary hydroxyl as “Tail”, and that with the secondary one as “Head”. Three signals from oxalate carbon atoms corresponding to HH, HT, and TT dyads could be found in the ^{13}C NMR spectrum, since all three types of dyads can form in the system (**Figure S4b**). In fact, three peaks were found in the 156-157 ppm region of the PPOx spectrum that was generated during a 24-hour period under equilibrium conditions (**Figure S4c**), which were significantly shifted downfield with respect to the monomer peak (**Figure S5**, 153.3 ppm). The middle peak was attributed to a HT dyad, while the side peaks represent symmetrical HH and TT dyads. The dyad distribution was close to random (0.59 : 1 : 0.47) that indicated the absence of regioregularity of the polymer chain. The degree of regioregularity was estimated from the ^{13}C NMR integral intensities as X_{reg} = [I(HH) + I(TT) – I(HT)]/[I(HH) + I(TT) + I(HT)]. The degree of regioregularity thus estimated was about 3% for PPOx isolated after achievement of polymerization equilibrium (**Figure S4c**). The low glass transition temperature (only about 16 ^{o}C) of the polymer, was consistent with the absence of regioregularity (**Figure S6**).[S7,S8]

The absence of regioregularity allows to assume that $k_{12}\approx k_{11}=k_1$, $k_{22}\approx k_{21}=k_2$. In other words, it does not matter which ester bond is attacked, it matters which OH-group attacks. The relative activity of terminal hydroxy end groups k_1 / k_2 turns to be equal to the ratio of the amount of secondary and primary OH groups in PPOx at equilibrium (1.5±0.1, **Figure 2b**).

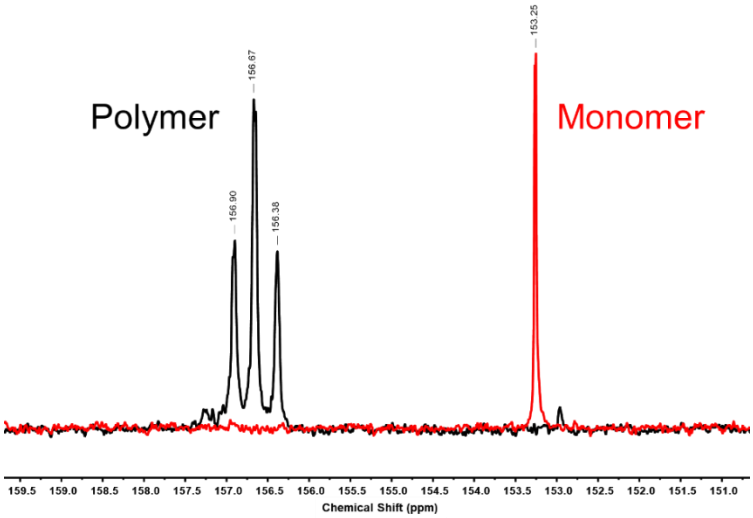

Figure S5. The fragments of ^{13}C NMR spectra of poly(propylene oxalate) obtained at 0.65% (mol.) of $Sn(Oct)_2$ (black) and cyclic propylene oxalate (red).

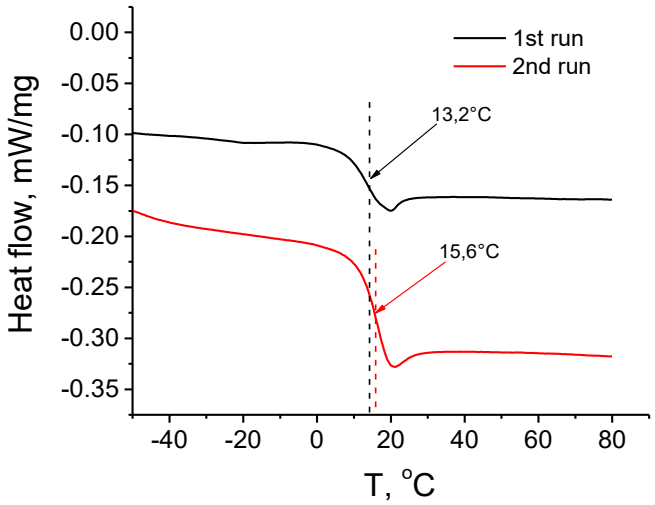

Figure S6. Differential scanning calorimetry of fractionated poly(propylene oxalate) (M_p = 8000, M_n ~ 5600). The black curve corresponds to the first scan at the rate 10 K·min^{-1}, the red curve corresponds to the second scan at the same rate. The threshold drop in heat capacity corresponds to the glass transition temperature, which equals to about 15.6 °C.

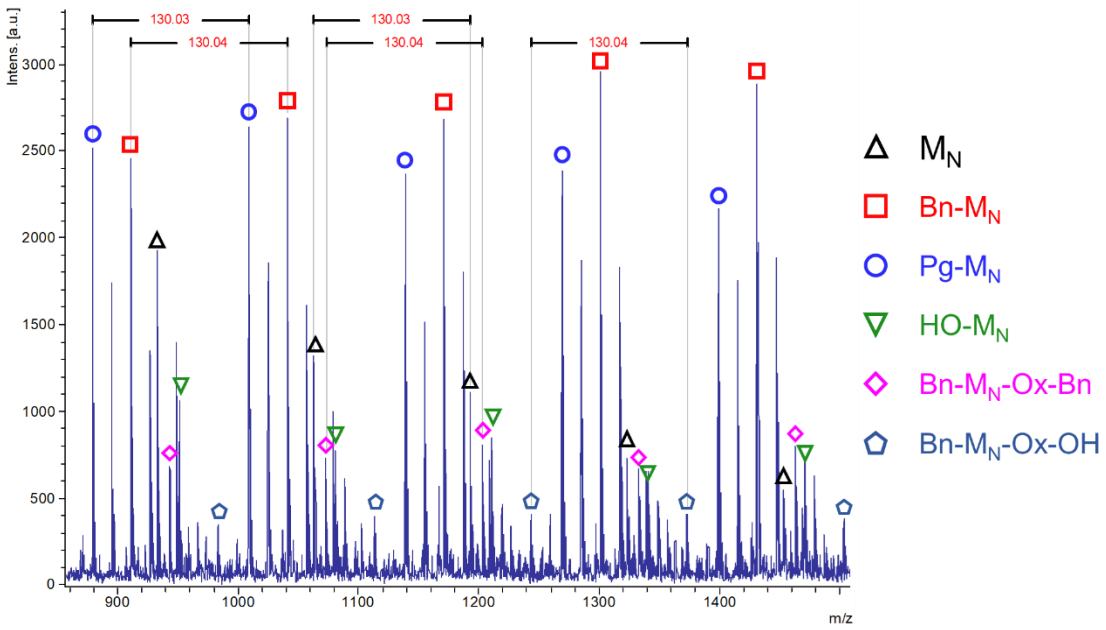

Figure S7. MALDI-TOF spectrum of reaction mixtures after PrOx polymerization in the presence of 0.65% (mol.) of $Sn(Oct)_2$ and 8.8%(mol.) of BnOH in respect to monomer at 100 °C during 24 h. Series of peaks are marked by colored shapes decoded in the right in accordance with **Figure 3** in the main text.

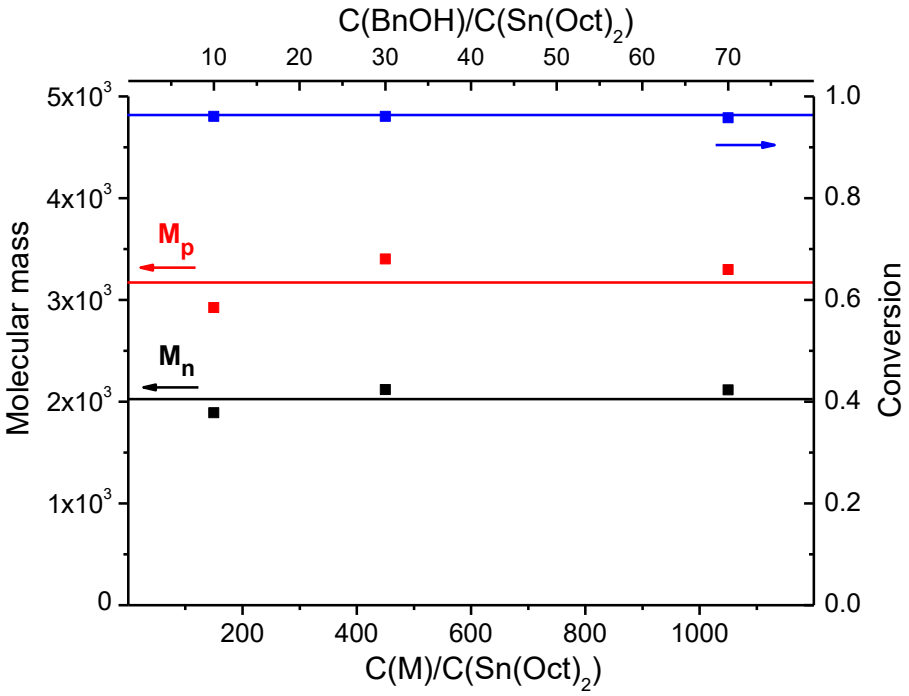

Figure S8. The most probable molecular masses of polymers determined by SEC (red), number average molecular masses of polymers determined by ^{1}H NMR (black) and polymerization conversions (blue) of polypropylene oxalate obtained by polymerization initiated with a constant amounts of BnOH [C(BnOH) = 6.7% (mol.)] in the presence of different amounts of $Sn(Oct)_2$ {C[$Sn(Oct)_2$] = 0.095-0.67% (mol.)}.

References

S1 N. P. Iakimov, E. M. Budynina, A. K. Berkovich, M. V. Serebryakova, V. B. Platonov, E. O. Fomin, A. G. Buyanovskaya, I. V. Mikheev and N. S. Melik-Nubarov, *Eur. Polym. J.*, 2024, **220**, 113410; https://doi.org/10.1016/j.eurpolymj.2024.113410.

S2 *AIST: Spectral Database for Organic Compounds, SDBS*: National Institute of Advanced Industrial Science and Technology (AIST), 2013, No.: 472, Spectral code: HR2012-02589NS; https://sdbs.db.aist.go.jp/SearchInformation.aspx.

S3 T. Iida and T. Itaya, *Tetrahedron*, 1993, **49**, 10511; https://doi.org/10.1016/S0040-4020(01)81546-5.

S4 C. A. DeRosa, A. M. Luke, K. Anderson, T. M. Reineke, W. B. Tolman, F. S. Bates and M. A. Hillmyer, *Macromolecules*, 2021, **54**, 5974; https://doi.org/10.1021/acs.macromol.1c00828.

S5 M. S. Ramesh and S. Rajaram, *Polymer*, 2021, **227**, 123803; https://doi.org/10.1016/j.polymer.2021.123803.

S6 P. Brignou, J.-F. Carpentier and S. M. Guillaume, *Macromolecules*, 2011, **44**, 5127; https://doi.org/10.1021/ma200950j.

S7 R. Xie, A. R. Weisen, Y. Lee, M. A. Aplan, A. M. Fenton, A. E. Masucci, F. Kempe, M. Sommer, C. W. Pester, R. H. Colby and E. D. Gomez, *Nat. Commun.*, 2020, **11**, 893; https://doi.org/10.1038/s41467-020-14656-8.

S8 H. Park, M. J. Han, Y. Kim, E. J. Kim, H. J. Kim, D. K. Yoon and B. J. Kim, *Chem. Mater.*, 2021, **33**, 3312; https://doi.org/10.1021/acs.chemmater.1c00466.